Journal of Power Sources 195 (2010) 2385–2392

Contents lists available at ScienceDirect

Journal of Power Sources

journal homepage: www.elsevier.com/locate/jpowsour

Lithium-ion battery cell degradation resulting from realistic vehicle and vehicle-to-grid utilization

Scott B. Peterson[a], Jay Apt[a,b], J.F. Whitacre[a,c,*]

[a] Department of Engineering and Public Policy, Carnegie Mellon University, Pittsburgh, PA 15213-3890, United States
[b] Tepper School of Business, Carnegie Mellon University, Pittsburgh, PA 15213-3890, United States
[c] Department of Materials Science and Engineering, Carnegie Mellon University, Pittsburgh, PA 15213-3890, United States

ARTICLE INFO

Article history:
Received 7 August 2009
Received in revised form 5 October 2009
Accepted 6 October 2009
Available online 10 November 2009

Keywords:
A123 systems
Li-ion battery
Vehicle-to-grid
Battery degradation
PHEV
LiFePO4
Vehicle battery testing profile

ABSTRACT

The effects of combined driving and vehicle-to-grid (V2G) usage on the lifetime performance of relevant commercial Li-ion cells were studied. We derived a nominal realistic driving schedule based on aggregating driving survey data and the Urban Dynamometer Driving Schedule, and used a vehicle physics model to create a daily battery duty cycle. Different degrees of continuous discharge were imposed on the cells to mimic afternoon V2G use to displace grid electricity. The loss of battery capacity was quantified as a function of driving days as well as a function of integrated capacity and energy processed by the cells. The cells tested showed promising capacity fade performance: more than 95% of the original cell capacity remains after thousands of driving days worth of use. Statistical analyses indicate that rapid vehicle motive cycling degraded the cells more than slower, V2G galvanostatic cycling. These data are intended to inform an economic model.

1. Introduction

One suggested benefit of plug-in hybrid electric vehicles (PHEVs) or battery electric vehicles (BEVs) is to provide electricity for off-vehicle use, "vehicle-to-grid" (V2G) services, when parked [1]. These benefits might include peak load shifting, frequency regulation and other ancillary services, smoothing variable generation from wind and other renewables, and providing distributed grid-connected storage as a reserve against unexpected outages. To determine the financial and technical feasibility of these applications, it is essential to quantify the effect of this kind of usage on battery degradation and performance. Most previous measurements have indicated that Li-ion battery capacity decreases as a result of cycling, and the magnitude of this loss is dependent on both the number of cycles and the depth of discharge (DoD) that the battery is subjected to during these cycles [2]. While these characteristics are well understood for the $LiNiCoO_2$/graphite-based cells used in the consumer electronics market (as well as for lead acid and NiMH systems), there is far less published data for the current and next generation of high rate cells that may see wide adoption in PHEV and BEV battery packs. Those data that have been published indicate it is possible to make Li-ion cells with much less capacity fade and dependence on depth of discharge than is commonly assumed [3]. However, these results are insufficient to determine the economics of V2G energy sales because they are from cycling that is not representative of battery use for driving and battery use for grid energy.

To provide more representative data, we examined the battery degradation of a battery cell already being implemented in the PHEV Hymotion battery pack (an aftermarket PHEV conversion), the A123 systems ANR26650M1 cell. We have examined the response of multiple sets of these cells (from different lots) to gauge their behavior in both simulated driving and combined driving/V2G energy sales modes. Our ultimate goal is to determine the performance and financial costs associated with cycling for V2G energy use in combination with a typical PHEV driving duty cycle. Simulating the actual discharge pattern also has enabled us to determine if there is a difference between dynamic discharge (representing the driving) and constant discharge (energy arbitrage) using statistical analyses.

2. Experimental

2.1. Driving profile created with data taken from NHTS

The energy arbitrage potential of a vehicle battery depends on both the usable capacity and the fraction of the pack used for daily

* Corresponding author at: Department of Materials Science and Engineering, Carnegie Mellon University, 3325 Wean Hall, 5000 Forbes Ave, Pittsburgh, PA 15213-3890, United States. Tel.: +1 412 268 5548.
E-mail address: whitacre@andrew.cmu.edu (J.F. Whitacre).

0378-7753/$ – see front matter © 2009 Elsevier B.V. All rights reserved.
doi:10.1016/j.jpowsour.2009.10.010

driving, while the lifetime cost of performing energy arbitrage will depend on how the pack degrades as a function of use mode. To experimentally quantify this, a nominal urban driving/V2G power profile and correlated battery test regime was derived by combing several common data sets. A representative urban commute driving duty cycle was constructed, using data from the 2001 National Household Travel Survey (NHTS) of 70,000 households [4]. To do this, we created a data set from the NHTS day trip file tabulating the daily trip profile of a vehicle. The day trip file contains "data about each trip the person made on the household's randomly assigned travel day" [5]. These trips include walking, taking public transportation, driving, or any other means of travel. We extracted only the trips taken by vehicles owned by households and eliminated trips taken at the same time by different members of the household in the same vehicle. This resulted in a new data set that tabulates the daily *vehicle* trips, instead of those of individual household members. The number of vehicles owned by the household is included in the day trip files, and only vehicles that were driven were used in the trip calculation.

The vehicle information data set was then cross-referenced to append vehicle-specific information, such as the age, fuel economy, and other relevant information. Vehicle-specific information was used to check for potential trends that might indicate that the NHTS data would not apply to PHEVs; none were found. Three cities in the Northeastern quadrant of the United States were selected: Boston (BOS), Philadelphia (PHL), and Rochester, NY (ROC). These cities were chosen because they are located in three different electricity markets and because they each had a high number of NHTS participants. The median number of trips taken on a given day by vehicles driven in each of the three cities was four (the mean was 4.46 for cities combined). For this reason, only vehicles which took four trips were thereafter considered in the determination of the representative profile. The median start time, duration, velocity, and distance of each trip in the three cities are listed in Table 1. Because the three cities had similar median trips, the data from all three cities were combined to make a single trip profile (Fig. 1). The total distance traveled was 29 km (original data in miles) when combining all four trips. This is similar to the result obtained if the same analytical steps are applied to the entire NHTS data set (total distance of 29 km; however trip start times and velocities vary).

2.2. Model constructed to replicate the energy use profile for driving

To determine the quantity and rate of energy transferred to and from a battery during driving conditions, we constructed a simple physics model that computed the energy needed to propel a typical vehicle through the NHTS trip profile. As an input to this model, the vehicle distance/velocity profile in each trip was created by sampling the Urban Dynamometer Driving Schedule (UDDS) and overlaying these segments into the average NHTS distance vs. time profile [6]. The 1370-s long UDDS profile was doubled in length to allow contiguous selections to span from the end of original UDDS profile to the beginning. These selections were portions of the UDDS profile, and significant fractions were repeated multiple times (Fig. 2).

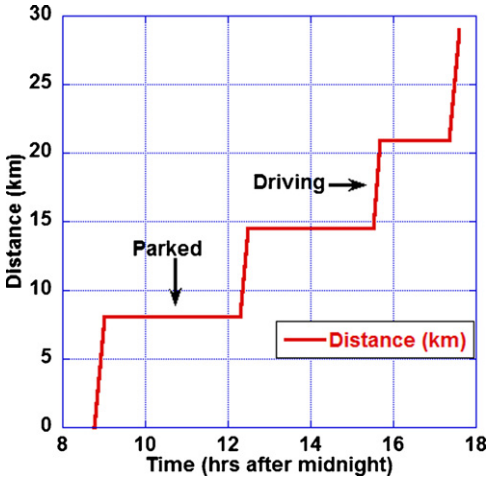

Fig. 1. The daily driving profile used in cell testing. This profile is an aggregate of data taken from all three cities included in study and represents all trips taken during the day (horizontal portions show when vehicle is parked, while diagonal portions represent driving).

To calculate the power vs. time battery duty cycle needed to achieve this velocity/acceleration profile, the vehicle was assumed to have the physical characteristics of a 2008 Toyota Camry; the mass was 1588 kg (3500 lbs), coefficient of drag of 0.28 and a frontal area of 2.7 m^2. The dimensionless coefficient of rolling resistance for the tires was assumed to be 0.01 [7]. This coefficient relates the resistance to movement as a function of normal force. The efficiency of power transfer from regenerative braking to batteries was assumed to be 40%, the efficiency from battery to wheels was assumed to be 80% [8]. The battery pack energy capacity was assumed to be 16 kWh (as in Chevrolet's proposed Volt) [9]. The density of air was taken from the US standard atmosphere at sea level.

An 800-W constant load was added to account for the power needed for all activities unrelated to movement such as heater, air conditioner, radio, lights and other accessories [10]. The total load

Table 1
Trip characteristics for three cities modeled and combined data used for battery testing.

City	Trip	Start time	Duration (min)	Average trip velocity (kph)	Distance (km)
BOS	1	8:48	14	38.6	7.2
	2	12:28	14.5	33.9	8.0
	3	15:00	10	32.2	6.4
	4	17:30	14.5	32.2	6.4
PHL	1	9:00	15	38.6	6.4
	2	12:04	11	38.6	6.4
	3	15:15	10	32.2	6.4
	4	17:00	15	32.2	8.0
ROC	1	8:43	15	45.1	9.7
	2	12:30	12	38.6	8.0
	3	15:40	10	38.6	6.4
	4	17:30	15	41.4	8.0
Combined	1	8:45	15	38.6	8.0
	2	12:16	12	38.6	6.4
	3	16:30	10	34.8	6.4
	4	17:20	15	38.6	8.0

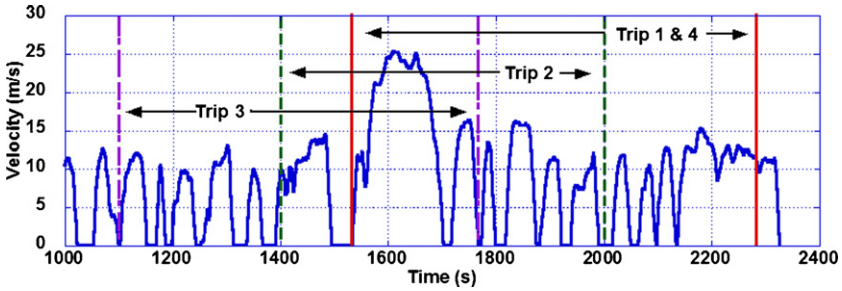

Fig. 2. Portions of urban dynamometer driving schedule (UDDS) were chosen to closely match driving profile shown in Fig. 1 in terms of duration and average velocity.

Table 2
Forces considered when calculating energy use for PHEV in charge depleting mode.

Force considered	Equation	Example: velocity = 10 m s^{-1} acceleration = 1 m s^{-2}
Acceleration	$F = ma$	1590 kg × 1 = 1590 N
Air resistance	$F_{ar} = 1/2\rho v^2 C_d A$	$1/2 \times 1.23\,\mathrm{kg\,m^{-3}} \times [10 m/s]^2\ 0.28 \times 2.67\,\mathrm{m^2} = 45.8$ N
Rolling resistance	$F_{rr} = C_{rr} mg$	0.01 × 1590 kg × 9.8 m s^{-2} = 156 N

every second was therefore obtained by adding the 800-W load to the power necessary to achieve the velocity defined in the UDDS. The force needed as a function of time to achieve the UDDS target speed is a summation of the forces listed in Table 2.

If the acceleration is sufficiently negative (indicating braking), that its absolute value is greater than air resistance and rolling resistance combined, then regenerative braking is occurring and the power values for motion are given by Eq. (1). The regenerative value will therefore be negative and indicates battery charging. Eq. (2) describes the necessary power for cases where no regenerative braking occurs:

$$\text{power} = \left(ma + \tfrac{1}{2}\rho v^2 C_d A + C_{rr} mg\right) 0.4 \times v \quad (1)$$

$$\text{power} = \frac{\left(ma + \tfrac{1}{2}\rho v^2 C_d A + C_{rr} mg\right) \times v}{0.8} \quad (2)$$

Using this model, we compute that the vehicle would use 31% of its battery pack capacity to drive the derived 4-trip profile, with 0.28 kWh/mile being withdrawn from the battery on average. This value appears reasonable; the Electric Power Research Institute's (EPRI) hybrid electric working group suggests 0.26 kWh/mile for a compact sedan [11].

The duty cycle profile derived from this model is used here as power-based "C-rate", the discharge power rate of a battery normalized to the total energy content. For example, for a 16 kWh battery a 16 kW load would be defined as having a discharge power with a 1 C-rate, 32 kW would be a 2 C-rate, etc. (in this case we are using power instead of the more common electronic current in Amps and Ah, for ease of calculation during economic analyses). By normalizing to cell energy and using a C-rate to determine power/current loads, the testing cycle can be run on any individual cell.

Under regenerative braking conditions, the battery pack will be charged if the deceleration provides more power than used by the constant base load (Fig. 3). The cumulative distribution of power levels over a driving cycle was calculated to illustrate the amount of time during the test cycle that the battery was under various loads (Fig. 4). The near-vertical portion is due to the base load that is constant when there is nearly no force required for motion. As a result of the relatively large energy-to-power ratio for a battery pack of this size, the absolute value of the C-rate imparted to the battery exceeds 1 only 20% of the time. The maximum absolute C-rate value was 2.85. This value is modest compared to the demonstrated rate capability of the tested cells, which are qualified by the vendor to a C-rate of at least 20C.

2.3. Cell acquisition and cycling

Thirteen cells were purchased at three separate times, and came from four different fabrication lots. Due to equipment limitations, testing start dates were staggered as new equipment became available. All testing was conducted with Arbin BT2000 series battery cyclers. The inception of testing of the first 4 cells (lot 1) was followed after 3 months by 4 more cells (lots 2 and 3), in turn followed

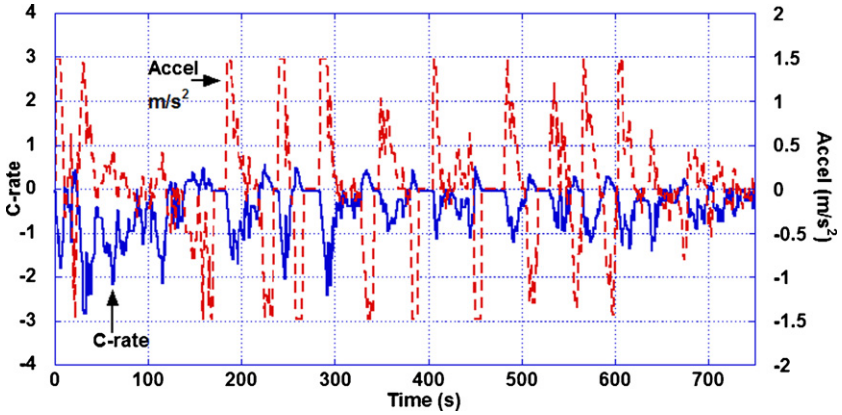

Fig. 3. Example of relationship between acceleration (red) and power required (in C-rate, blue) for trips 1 and 4. A negative C-rate corresponds to discharge rate from pack. Deceleration can lead to regenerative braking if it is significant—in this case, around 7% of the energy is regained via regenerative braking.

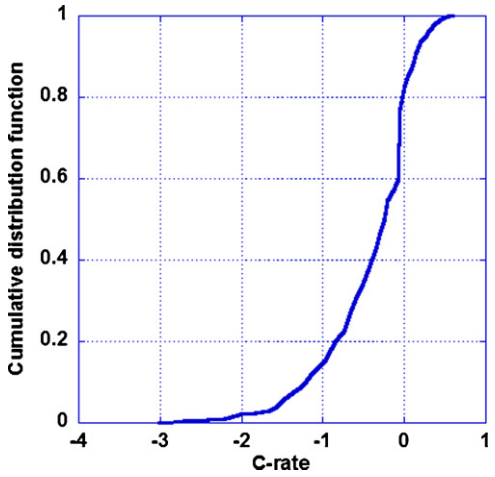

Fig. 4. Cumulative distribution function of power requirements for daily driving (all four trips). Given large pack size the current rates are low most of the time. The near-vertical portion is a result of times when velocity and acceleration are low and the base load to run accessories dominates the power needs for vehicle.

by 5 more cells (lot 4) after another 4 months. Cells from lot 1 underwent 2400 cycles, lots 2 and 3 completed 2000 cycles and lot 4 had reached 1000 cycles when this paper was submitted. Again, each cycle in this case represents a single driving day, so some of these cells were tested the equivalent of at least 5 driving years.

The cells were not thermally controlled and were kept at the lab ambient temperature, which varied from 24 to 27 °C, but was most commonly approximately 25 °C. Data published by the manufacturer indicating good cell stability and uniformity up to at least 40 °C imply that the cell temperatures used in this testing were not high enough to cause excess degradation, nor were they variable enough to significantly affect the data [12]. A thermocouple was connected to one cell and temperature was monitored though several full driving cycles; the cell temperature did not increase significantly, as expected from these cells, which have been engineered for high rate applications and so do not heat up significantly under the nominally low C rates experienced.

The cells were subjected to one of five different driving day testing cycles. Test cycle 1 corresponded to driving only and is shown in Fig. 5, while each of the other 4 cycles consisted of the same daily duty cycle, with varying amounts of additional V2G discharge in the afternoon hours. The V2G discharge consisted of a specific time at a galvanostatic C/2 rate (1.15 A in this case), and in and a cutoff voltage of 2.5 V was used to avoid over-discharge. A C/2 discharge rate was chosen to represent V2G simulation because it scales to an approximate 8 kW rate of withdrawal from the 16 kWh pack. The rate might be forced lower depending on the infrastructure available in the home; a 240 V, 30 A circuit could maintain only 7.2 kW of energy transfer. This implies the rate of discharge will likely be below C/2 slightly unless a special circuit is installed. Each cycle began with a 1C galvanostatic charge of 2.3 A until cells reached a voltage of 3.6 V followed by a 5 min rest. Then trips 1–3 were executed with 5 min rests between each. The V2G discharge then was conducted. The driving only cells had no V2G discharge (3 cells, one each from lots 1, 2, and 4). Test cycle 2 had one V2G discharge of 1.15 A for 995 s (3 cells, one each from lots 1, 2, and 4). Test cycle 3 had one V2G discharge lasting 1715 s (3 cells, one each from lots 1, 2, and 4). Test cycle 4 had 2 V2G discharges and was the same as test cycle 3 with an additional V2G discharge after trip 4 held until the cell voltage dropped to 3.2 V (3 cells, one each from lots 1, 3 and 4). Test cycle 5 extended the second V2G discharge until 2.5 V (1 cell from lot 4). This test regimen is indicated in Table 3.

Table 3
Testing regimens used on cells.

Test cycle	Length of first V2G discharge (s)	Voltage at end of second V2G discharge
1	0	NA
2	995	NA
3	1715	NA
4	1715	3.2
5	1715	2.5

The duration of the rest period the end of each driving day simulation was adjusted such that each test case, regardless of the degree of V2G discharge, lasted 3 h. This regimen was repeated for 100 cycles, and then the cells were put through a C/2 charge/discharge "measurement" cycle to 100% state of charge/discharge to measure cell capacity. This started with charging the cell 1.15 A until it reached a voltage of 3.6 V. Then the voltage was held constant until the current tapered to 0.01 A to ensure the cells were fully and equally charged. After a 5-min rest the cells were discharged at 1.15 A rate until voltage fell below 2.5 V (i.e. 100% DoD). The capacity measured through this discharge was defined as the cell capacity at that point in the testing. To avoid biasing the results with differing rest periods between test cycle and baseline cycle the baseline check automatically began 5 min after completion of the 100 test cycles.

3. Results and analyses

The cells from different lots did not behave identically. Lot 1 showed a significant degree of variation in capacity retention as the

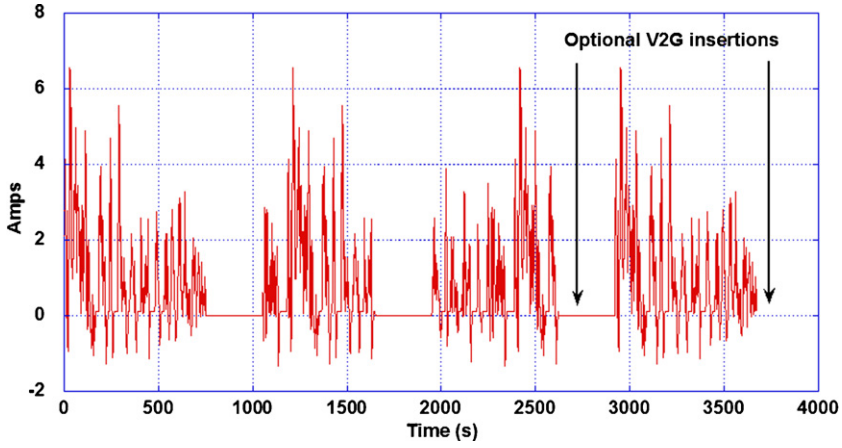

Fig. 5. Test current profile used to simulate driving day for cells showing all trips. The times after trips 3 and 4 when V2G discharge was simulated are indicated.

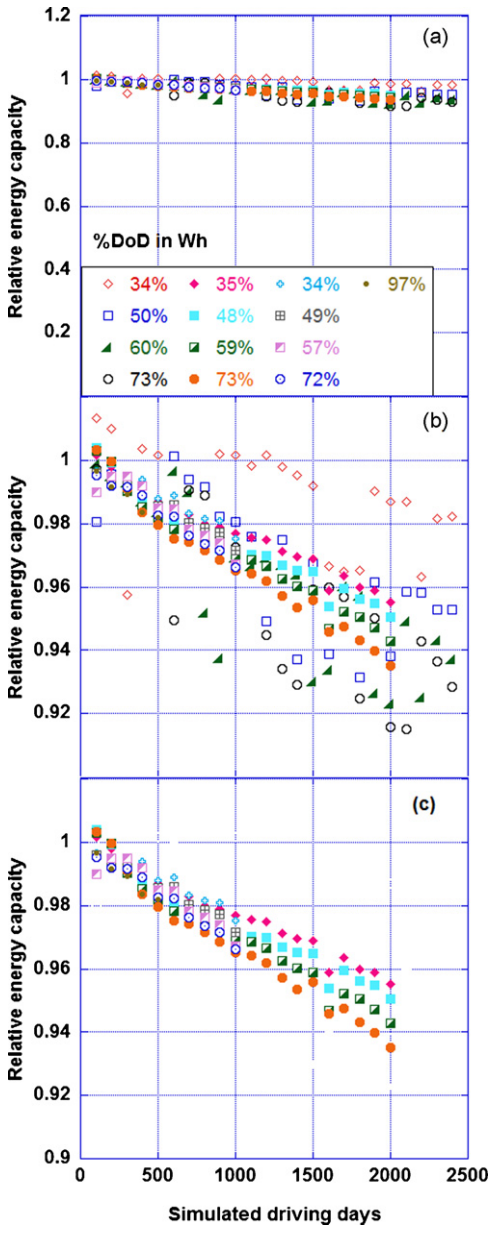

Fig. 6. Degradation of cells vs. driving days simulated (a) full range, (b) same information zoomed and (c) with highly variable cells from lot 1 dropped.

cells were cycled (Fig. 6a and b), with cells increasing and decreasing in capacity as they were cycled, although the overall trend was downward. Lots 2–4 showed remarkable consistency in degradation (Fig. 6c). It is possible that the unusual scatter observed in the data from lot 1 is somehow linked to the integrity of the BT2000 test unit used for these cells (on which only these 4 cells have been tested), though such a link has not been quantified. For this reason they are not used in the final statistical analysis.

Because the cells from different lots might have undergone different formation (at the factory) before testing started it was necessary to find a way to determine an initial capacity in a consistent manner. One common approach is to measure capacity after a specific number of identical low rate cycles. We considered this unsuitable because we felt it was desirable to avoid running a large number of cycles on the battery in an attempt to normalize them and thus decrease capacity by an unknown amount. The next alternative we considered was to measure the capacity after an arbitrary number of cycles, but with five different possible test cycles this

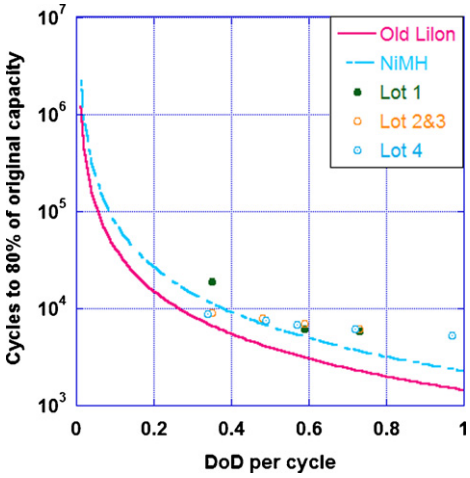

Fig. 7. Laboratory results overlaid onto VARTA curves illustrating more linear response in cycle life as a function of depth of discharge for the cells tested.

was also unsatisfactory. Instead, we performed a linear regression on each cell data set to back-predict their initial capacity in terms of cycles tested. The short prediction range made this an acceptable solution because any deviations from the true value would not affect the prediction strongly. Indeed, predicted initial values were close to measured initial values in most cases. This capacity was then used to determine the relative loss as a function of cycles instead of using a numerical value for the total energy content. A linear regression of relative capacity degradation vs. cycles was then used to predict when the cell would reach 80% of original capacity. This information was used to predict the cycle life vs. DoD/cycle.

Overlaying the values on the VARTA Automotive plot shows that DoD/cycle appears to have a smaller effect on degradation with these cells compared to those reported previously, particularly given that a single "cycle" in this case was representative of an entire day's worth of driving. This appears to indicate that the portion of a cell's capacity used, or the ultimate depth of discharge, is not as important with A123 systems based cells as with the cells on VARTA plot labeled old Li-ion and NiMH (Fig. 7), where DoD is a key variable [13]. As the degree of discharge per driving day increases, the predicted cycle life does not fall as rapidly as conventional data analysis commonly predicts. For example, in cells discharged to 95% DoD per cycle, our measurements predict that 5300 cycles will be needed before reaching 80% of initial capacity instead of around 1500 cycles as indicated by the VARTA data. Also, daily cycles with shallower DoD values do not appear to increase cycle life as significantly as those indicated from the VARTA analyses. This suggests that a greater portion of the cell capacity could be used during each cycle than would be suggested by the VARTA plot if applied to this chemistry.

Fig. 8 shows data for a C/2 discharge of the same cell (from lot 3) after 0, 1000, and 2000 simulated driving days. The potential profile in the voltage plateau region was essentially unchanged after 2000 cycles, indicating that internal resistance did not change significantly, as the differential in cell polarization under discharge before and after the 2000 cycles was imperceptible. The decrease in delivered capacity after cycling is manifested as a departure from the discharge plateau after 1.82 Ah of discharge for the heavily cycled cell vs. 1.91 Ah for the uncycled cell (Fig. 8b).

The test profiles used on these cells were very different from those typically published (i.e. potential-limited galvanostatic charge/charge at intermediate rates), so a different approach is used here to quantify the capacity fade as a function of battery use. Simple accounting for the %DoD at end-of-cycle DoD does not accurately represent the amount of energy processed by a

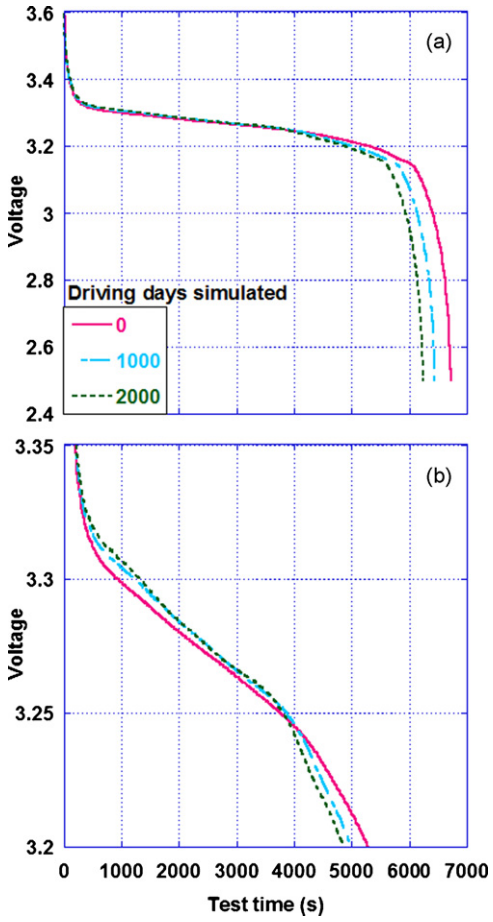

Fig. 8. Voltage profiles of a cell that reached an ultimate DoD value of 73% each driving day. The initial, 1000th and 2000th baseline discharge curves are shown.

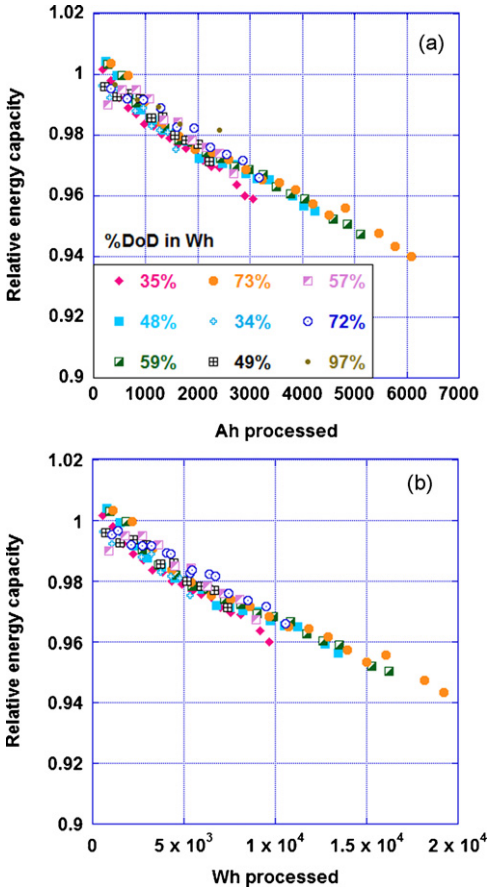

Fig. 9. Degradation as a function of (a) capacity (Ah) processed by cell or (b) energy (Wh) processed by cell for all but lot 1 cells. Both appear linearly related, as expected given the nominally linear discharge profile of the $LiFePO_4$/graphite system.

cell per cycle. For example, the ratio of charging from regenerative braking to discharging produced by the model was 0.076; if 100% energy efficiency is assumed, then at least 14% more energy is exchanged during a driving cycle beyond the energy associated with the indicated DoD value. To this end, percent initial capacity was related to the total capacity (in Ah) processed by each cell, a value that included the discharge for driving, charging from regenerative braking, charging during the evening to recharge the battery for the next day, baseline check. This value can be directly related to the moles of Lithium ions transferred between the electrodes during use.

Data collected from cell lot 1 showed inconsistencies, again, consistent with the capacity vs. cycle life for these cells. However, the second set of cells, lots 2–4, showed a high level of consistency in degradation with respect to integrated Ah processed; the cells appear to degrade in response almost exclusively to capacity processed as opposed to the number of cycles, or the DoD per cycle (Fig. 9a). The sample analysis based on energy processed (in Wh) showed marginally better results and were more directly applicable to modeling the energy arbitrage potential of the cells (Fig. 9b). There appeared to be a slight difference in slope between cells. Those with greater energy arbitrage discharge appeared to degrade slightly slower. Comparing two specific cells from lot 2 over a similar range of energy processed shows a different but statistically insignificant slope (at the 95% level) (Fig. 10). Adding cells from lot 4 tightens the 95% confidence interval lessening the overlap of the two slopes, at the 95% level, but they are still not statistically different.

To investigate this further, a multiple linear regression was conducted to relate the degradation of the cells to the type of cycling incurred. The first step was to break the total Wh processed by each cell in different categories of charge and discharge. It was assumed that these different cycling regimes could be represented by driving discharge, driving recharge (from regenerative braking), energy arbitrage discharge, and recharge. The first two are dynamic, while

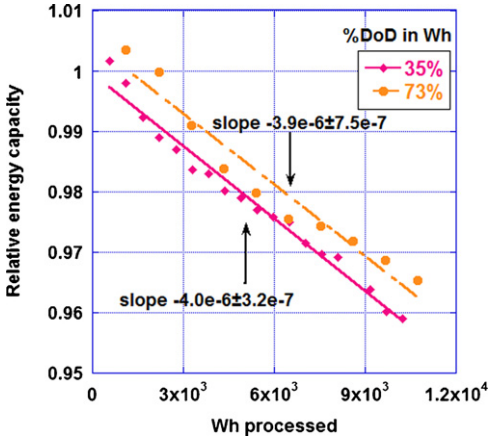

Fig. 10. Capacity degradation as a function of energy processed for two cells tested with contrasting end-of-cycle depth of discharge values (35% and 73% DoD). The slight observed difference would indicate less degradation for higher DoD/cycle cell, however the 95% confidence interval of slopes overlaps for these fits, so they are not statistically discernable.

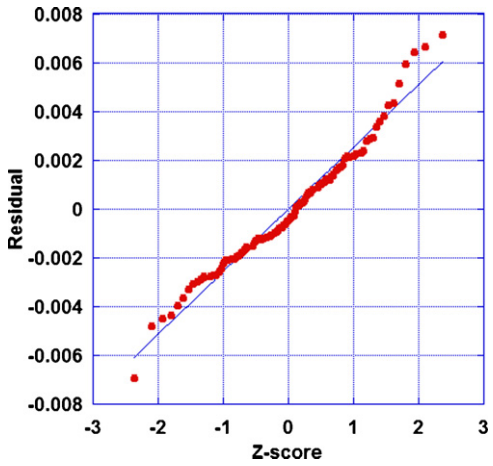

Fig. 11. Q–Q plot shows errors are normally distributed for multiple linear regression. The line represents expected values for a normal distribution.

the last two categories are constant rate. The values were normalized to the initial capacity of each cell to remove variation from differing initial capacity. Regenerative braking recharge was highly correlated with the driving discharge because the simulation had a specific ratio of regenerative braking to driving discharge as defined by the UDDS. Therefore, regenerative braking was dropped from the multiple linear regression analysis. Only driving discharge and energy arbitrage discharges were considered for the multiple linear regression, because the other values could be almost perfectly predicted if these values were known. The errors of the resulting regression appear to follow the assumption of normality, as shown in Fig. 11, which indicates that a multiple linear regression can be used without fear that the errors follow a pattern that would indicate some hidden underlying process [14].

The resulting regression appeared linear (adjusted $R^2 = 0.96$). The relative size of the coefficients implies that the battery usage associated with driving causes more loss in cell capacity per Wh processed than usage associated with V2G load shifting (constant rate and polarity) (Table 4). The confidence intervals are small enough that there is no overlap as indicated by the high absolute value of the *t*-stat. The regression relates percent capacity loss to energy discharged driving, energy discharged for arbitrage, and initial capacity. An example is shown in Table 5, where we illustrate how a given quantity of energy processed in a particular mode can be used to predict the percent capacity loss. Because all cells underwent the same cycling associated with driving, the differences in these coefficients relates not just to the difference in degradation from dynamic discharge vs. constant discharge, but also to other hidden variables such as cell aging, which is thought to be minimal over the approximately 12 months of testing performed for this study [15].

Table 4
Results of multiple linear regression.

Coefficient	Value	*t*-Stat	Confidence interval
Wh discharged driving	−5.99E−5	−34.9	1.71E−6
Wh discharged arbitrage	−2.71E−5	−14.6	1.85E−6
Constant	1.00	2120	4.7E−4

Table 5
Example using results of multiple linear regression to calculate battery capacity degradation.

Coefficient	Value	Normalized	Multiplied by coefficient
Wh discharged driving	3000 Wh	462	−0.027
Wh discharge arbitrage	1500 Wh	231	−0.0062
Initial capacity	6.5 Wh	1	
Capacity remaining	97%		

4. Discussion/conclusions

The loss of capacity as a function of driving days shown in Fig. 6 indicates that the degradation of these high-power $LiFePO_4$-based cells does not follow the same pattern as commonly used previous reported results and models [16,17]. These data reveal that in benchtop testing of simulated driving conditions, the cell DoD does not have nearly as great an effect on lifetime as previously reported values for other battery chemistries (commonly those based on layered metal oxide cathodes such as $LiMO_2$ where M is some combination of Co, Ni, and Mn) [14,15,18]. This result implies that a $LiFePO_4$/graphite-based PHEV battery pack with properly matched cells can be cycled though a very broad state of charge range without incurring any significant increase in capacity loss as a function of Ah or Wh processed. In principle, a PHEV can utilize a smaller battery and use a greater proportion of the battery, however doing so might make discharge rate and associated ohmic heating more of an issue.

After 2000 cycles the low rate discharge potential profile appears very similar to that collected before cycling started, and a very small fraction of the initial capacity has been lost. This observation is consistent with the hypothesis that only a minimal Solid Electrolyte Interphase (SEI) layer must be forming during cycling of these cells, and that the mechanical cycling of the electrodes does not induce loss of connection and capacity fade. The tendency for increased I^2R cell heating after many cycles is not present (due to the relatively low C-rates encountered), and so failure mechanisms associated with this effect are minimal.

The comparison between capacity fade as a function of cycle number and Ah processed provides several key insights to the processes at work in these batteries. First, the dominant cell degradation method is not dependant upon depth of discharge, or rate of discharge (at least up to the 3C spikes encountered in this test regimen). For example, if only the data shown in Fig. 6 were used to examine capacity loss, the conclusion might be drawn that degradation was indeed a function of depth of discharge. However, we show in Fig. 9 that, in fact, the cycle DoD and relative fraction of low-rate galvanostatic cycling vs. acceleration/regenerative braking current pulses are not important even over thousands of driving days. Rather, it is the integrated number of lithium ions that have been intercalated/de-intercalated into the electrodes, regardless of the DoD at which these events occur. Nevertheless, there are still other factors of importance. The multiple regression shows there is a difference between driving energy withdrawn and constant discharge. With the low rate constant discharge associated with roughly half the degradation of the dynamic discharge (−6.0E−3% and −2.7E−3% for 1 normalized Wh). For this reason, using constant discharge degradation to predict driving degradation is likely inaccurate, and correction factor attributed to the kind of cycling encountered is prescribed.

The literature commonly indicates that the dominate mechanisms for capacity loss in Li-ion cells are (1) the formation of a resistive and progressively Li-consuming interfacial layer between the functional graphite at the anode and the electrolyte, and (2) the physical degradation of active materials and electrode structures [19]. Our data indicate a much lower loss of capacity as a function of cycles and Ah processed, a result consistent with the use of high performance nano-structured electrode (cathode) materials that are much more physically stable during use and so do not degrade. The remaining loss in capacity is likely due to anode interfacial film of $Li_2O/LiF/Li_2CO_3$/other formation [20]. In most interpretations, the

loss of capacity is correlated to amount of Li that has reacted to form the SEI and so is no longer functional in the battery function. The fact that we observed little to no relationship between DoD and capacity fade supports the idea that the SEI formation at the anode occurs at the same rate regardless of state of charge and degree of graphitic lithiation. A recent capacity degradation model is consistent with this hypothesis; the anode potential was not varied significantly during simulation and so depth of discharge was not nearly as important as the time-integrated current of Li-ions the SEI was driven to process during cycling [17]. Higher rate cycling causes more rapid capacity loss. This is also consistent with the literature in several ways: at higher rates greater overpotentials are observed at the electrode surfaces and will therefore slightly enhance the rate SEI formation. Local heating at the electrode surface at high rates could also increase the rate of SEI formation. It should also be noted that the cells were kept at room temperature throughout the test mainly for convenience. It is acknowledged, however, that the rate of capacity loss would almost certainly have been greater for cells kept at elevated temperatures during testing. Elevated and variable temperature testing will be conducted in our labs to explore this possibility.

5. Summary

The composition of a test "cycle" is important when quantifying battery degradation, and using depth of discharge (DoD) per cycle as an independent variable when studying capacity fade can be misleading in cases where each cycle is laden with rapid discharge and charge events. Analyses performed here show that the strongest indicator of capacity fade for the type of cell tested (A123 systems M1 Cell) was the integrated capacity or energy processed, regardless of the DoD experienced. Furthermore, statistical analyses show that using a PHEV battery for V2G energy incurs approximately half the capacity loss per unit energy processed compared to that associated with more rapid cycling encountered while driving, and DoD was not important in either case except as a reflection of energy processed. The percent capacity lost per normalized Wh or Ah processed is quite low: -6.0×10^{-3}% for driving support and -2.70×10^{-3}% for V2G support. These values show that several thousand driving/V2G driving days incur substantially less than 10% capacity loss regardless of the amount of V2G support used. However, V2G modes that are more intermittent in nature will lead to more rapid battery capacity fade and should be avoided to minimize battery capacity loss over many years of use.

List of symbols

PHEV	plug-in hybrid electric vehicle
BEV	battery electric vehicle
V2G	vehicle-to-grid energy transfer
NHTS	National Household Transportation Survey
BOS	Boston, MA
ROC	Rochester, NY
PHL	Philadelphia, PA
UDDS	Urban Dynamometer Driving Schedule
kWh	kilowatt hours
m	mass
a	acceleration
ρ	density of air
v	vehicle velocity
C_d	coefficient of drag
A	frontal area of vehicle
C_{rr}	dimensionless coefficient of rolling resistance
g	acceleration of gravity
Δt	time step in s
V	volt
A	amp
DoD	depth of discharge

Acknowledgements

The authors thank Paul F. Fischbeck and Lester B. Lave for helpful discussions. This work was funded in part by the National Energy Technology Laboratory of the Department of Energy, the Alfred P. Sloan Foundation and the Electric Power Research Institute under grants to the Carnegie Mellon Electricity Industry Center (CEIC), and the U.S. National Science Foundation through the Climate Decision Making Center at Carnegie Mellon University under grant SES-0345798. This manuscript does not necessarily reflect the views of any of the funding agencies. No funding agencies had any role in the collection, analysis or interpretation of data; in the writing of the report; or in the decision to submit the paper for publication.

References

[1] W. Kempton, S.E. Letendre, Electric vehicles as a new power source for electric utilities, Transport. Res. 2 (1997) 157–175.
[2] A.G. Ritchie, Recent developments and likely advances in lithium rechargeable batteries, J. Power Sources 136 (2004) 285–289.
[3] J. Axsen, A. Burke, K. Kurani, Batteries for Plug-in Hybrid Electric Vehicles (PHEVs): Goals and the State of Technology Circa 2008, Institute of Transportation Studies University of California Davis, 2008.
[4] U.S. DoT, National Household Travel Survey, http://nhts.ornl.gov/download.shtml (2001).
[5] U.S. DoT, 2001 National Household Travel Survey: User's Guide, 6-2, http://nhts.ornl.gov/publications.shtml#usersGuide (2004).
[6] Epa, Urban Dynamometer Driving Schedule, http://www.epa.gov/nvfel/methods/uddscol.txt.
[7] T.R. Board, Tires and passenger vehicle fuel economy: informing consumer, Improv. Perform. (2006).
[8] N. Demirdöven, J. Deutch, Hybrid cars now, fuel cell cars later, Science 305 (2004) 974–976.
[9] B. Stewart, GM Testing Volt's Battery, iPhone-like Dash on Track to 2010, Popular Mechanics (2008), http://www.popularmechanics.com/automotive/new_cars/4257460.html.
[10] R. Farrington, J. Rugh, Impact of Vehicle Air-Conditioning on Fuel Economy, Tailpipe Emissions, and Electric Vehicle Range (2000) http://www.nrel.gov/docs/fy00osti/28960.pdf.
[11] M. Duvall, Comparing the Benefits and Impacts of Hybrid Electric Vehicle Options for Compact Sedan and Sport Utility Vehicles (2002). http://mydocs.epri.com/docs/public/000000000001006892.pdf.
[12] High Power Lithium Ion ANR26650M1A, http://a123systems.textdriven.com/product/pdf/1/ANR26650M1A_Datasheet_APRIL_2009.pdf.
[13] M. Duvall, Batteries for Plug-in Hybrid Electric Vehicles, Presented at Seattle Electric Vehicle to Grid (V2G) Forum (2005) 5. http://www.ceoe.udel.edu/cms/wkempton/Kempton-V2G-pdfFiles/PDF%20format/Duvall-V2G-batteries-June05.pdf.
[14] D.S. Moore, G.P. McCabe, Introduction to the Practice of Statistics, 4th ed., Freeman, NY, 2003, p. 722–723.
[15] http://www.a123systems.com/technology/life.
[16] I. Bloom, et al., An accelerated calendar and cycle life study of Li-ion cells, J. Power Sources 101 (2001) 238–247.
[17] G. Ning, R.E. White, B.N. Popov, A generalized cycle life model of rechargeable Li-ion batteries, Electrochim. Acta 51 (2006) 2012–2022.
[18] M. Broussely, et al., Main aging mechanisms in Li ion batteries, J. Power Sources 146 (2005) 90–96.
[19] Broussely, et al., Multimodal physics-based aging model for life prediction of Li-ion batteries, J. Electrochem. Soc. 156 (2009) A145–A153.
[20] D. Aurbach, Review of selected electrode-solution interactions which determine the performance of Li and Li ion batteries, J. Power Sources 89 (2000) 206–218.